Separation Science and Technology
Publication details, including instructions for authors and subscription information:
http://www.informaworld.com/smpp/title~content=t713708471

Selective Removal of Cesium from Sodium Nitrate Solutions by Potassium Nickel Hexacyanoferrate-Loaded Chabazites

Hitoshi Mimura[a]; Masanori Kimura[a]; Kenichi Akiba[a]; Yoshio Onodera[b]
[a] INSTITUTE FOR ADVANCED MATERIALS PROCESSING, TOHOKU UNIVERSITY, SENDAI, JAPAN [b] TOHOKU NATIONAL INDUSTRIAL RESEARCH INSTITUTE, SENDAI, JAPAN

Online publication date: 01 November 1999

To cite this Article Mimura, Hitoshi , Kimura, Masanori , Akiba, Kenichi and Onodera, Yoshio(1999) 'Selective Removal of Cesium from Sodium Nitrate Solutions by Potassium Nickel Hexacyanoferrate-Loaded Chabazites', Separation Science and Technology, 34: 1, 17 — 28
To link to this Article: DOI: 10.1081/SS-100100633
URL: http://dx.doi.org/10.1081/SS-100100633

SEPARATION SCIENCE AND TECHNOLOGY, **34**(1), pp. 17–28, 1999

Selective Removal of Cesium from Sodium Nitrate Solutions by Potassium Nickel Hexacyanoferrate-Loaded Chabazites

HITOSHI MIMURA, MASANORI KIMURA, and KENICHI AKIBA
INSTITUTE FOR ADVANCED MATERIALS PROCESSING
TOHOKU UNIVERSITY
KATAHIRA-2, AOBA-KU, SENDAI 980-8577, JAPAN

YOSHIO ONODERA
TOHOKU NATIONAL INDUSTRIAL RESEARCH INSTITUTE
NIGATAKE-4, MIYAGINO-KU, SENDAI 983-0036, JAPAN

ABSTRACT

Potassium nickel hexacyanoferrate(II)s (KNiFC) were incorporated in the porous matrix of chabazite by successive impregnation with $Ni(NO_3)_2$ and $K_4Fe(CN)_6$. The loading percentage of KNiFC crystals on chabazite increased with repeated times of impregnation. The ion-exchange equilibrium of Cs^+ in KNiFC-loaded chabazite (CFC) was attained within 2 days. Relatively large distribution coefficients of Cs^+, $K_{d,Cs}$, above 10^4 cm^3/g were obtained, irrespective of coexisting $NaNO_3$ concentration. There is a large difference between the K_d value of ^{137}Cs and those of other nuclides; the separation factor of Cs/Sr ($\alpha_{Cs/Sr} = K_{d,Cs}/K_{d,Sr}$) was estimated to be above 10^4. The breakthrough curve for Cs^+ through the column packed with CFC exhibited a symmetrical S-shaped profile, and this exchanger proved to be effective for the selective removal of radiocesium from waste solutions containing highly concentrated $NaNO_3$.

INTRODUCTION

Special attention has been given to the selective removal of ^{137}Cs from radioactive waste solutions containing highly concentrated $NaNO_3$ in relation to the reduction of the volume of wastes and the partitioning of radioactive nuclides (1, 2). Among various inorganic ion-exchangers exhibiting high se-

lectivity to Cs^+, insoluble hexacyanoferrates have been employed for the removal of ^{137}Cs in the treatment of radioactive waste solutions (3–5).

Potassium nickel hexacyanoferrate(II)s (KNiFC) can be obtained readily by precipitating $Ni(NO_3)_2$ with $K_4Fe(CN)_6$ (6–10). While these products are composed of aggregates of very fine (about 30 nm in diameter) crystals and have low mechanical stability, the precipitates of KNiFC tend to become colloidal in aqueous solution and are unsuitable for practical applications such as column operation. In order to improve their mechanical properties, the preparation of ferrocyanides exchangers has been carried out by precipitation on solid inert supports such as silica gels and bentonites (11–15). However, the preparation procedures were rather complicated and the results were often not reproducible.

Chabazite, a kind of natural zeolite with a relatively large void volume (16) and a specific surface area, is available as a carrier of microcrystalline ferrocyanides. This zeolite is a selective ion-exchanger for Cs^+ and has a relatively large distribution coefficient ($K_{d,Cs}$) of about 10^4 cm^3/g in the presence of $NaNO_3$ up to 0.1 M. The $K_{d,Cs}$ for chabazite tends to decrease markedly with increasing Na^+ concentration above 1 M (17). In this study we attempted to incorporate KNiFC crystals into the porous support of chabazite by successive impregnation of macropores with $Ni(NO_3)_2$ and $K_4Fe(CN)_6$ solutions.

The present paper deals with the procedure for the preparation of KNiFC-loaded chabazites and the selective removal of ^{137}Cs from highly concentrated $NaNO_3$ solutions.

EXPERIMENTAL

Procedure for Preparation

The procedure for the preparation of KNiFC-loaded chabazite (CFC) is shown in Fig. 1. The unit cell content of chabazite used as a porous carrier was $Ca_2[(AlO_2)_4(SiO_2)_8]\cdot 13H_2O$ (Linde IE-96). Two grams of chabazite dried at 200°C was contacted with a 20-cm^3 solution of 1 M (mol/dm^3) $Ni(NO_3)_2$ under reduced pressure at 25°C for 3 hours and then washed with acetone and air-dried at 90°C for 3 hours. In a similar manner, chabazite impregnated with $Ni(NO_3)_2$ was reacted with a 20 cm^3 solution of 0.5 M $K_4Fe(CN)_6$ to form KNiFC precipitates in the macropores of chabazite. The single-loaded chabazite (designated as CFC-I) was washed with deionized water and acetone, air-dried at 90°C for 3 hours, and finally stored in a sealed vessel over a saturated NH_4Cl solution (humidity: 79% at 25°C) at a constant vapor pressure of water. The double-loaded and triple-loaded samples, CFC-II and CFC-III, were prepared by repetition of the above procedure.

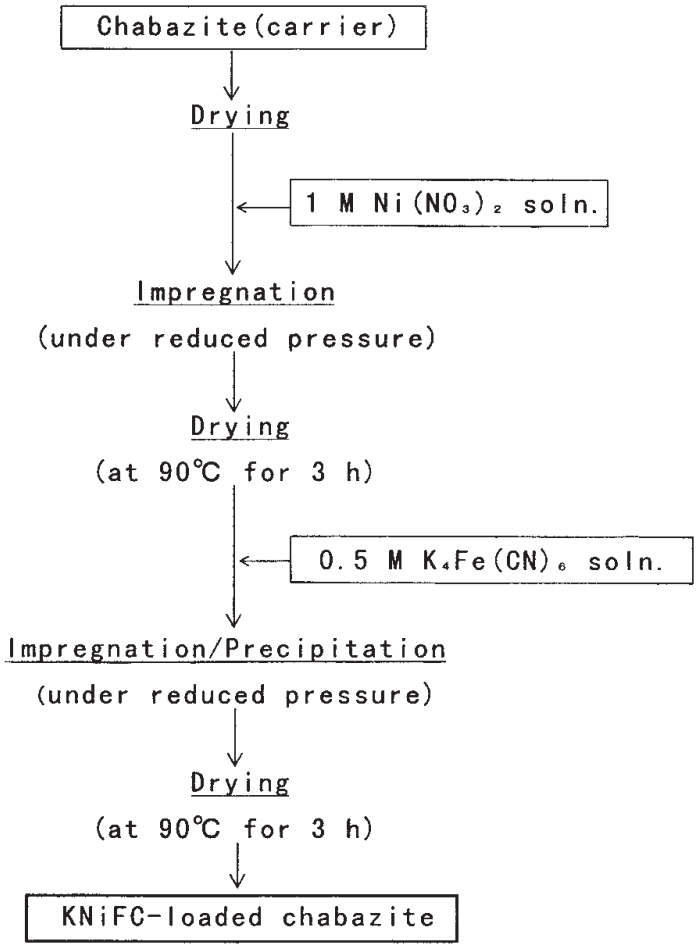

FIG. 1 Procedure for the preparation of KNiFC-loaded chabazite.

The structure of CFC was determined by powder x-ray diffractometry (XRD, Rigaku RAD-B) using monochromatized CuKα radiation. The loading percentage and chemical composition of CFC were determined by electron probe microanalysis (EPMA, Hitachi X-650S). The loading percentage was defined as the weight percentage (wt%) of KNiFC crystals in the CFC products. The chemical composition of KNiFC was calculated by taking the amount of irons as unity and normalizing the nickel amount to this value. The proportion of potassium was then calculated on the basis of the iron and nickel values and assuming electrical neutrality. Surface morphologies were examined by scanning electron microscopy (SEM). The cyano group in KNiFC was checked by the KBr method, using an infrared spectrophotometer (Hitachi 260-50); the optical density (D, $D = \ln I_0/I$) of the absorption band of C≡N at 2,100 cm^{-1} was estimated.

Determination of Distribution Coefficient

The distribution coefficients of various radioactive nuclides were determined by the batch method. An aqueous solution (7 cm^3) containing 10 ppm metal ion labeled with a radioisotope was contacted with 0.070 g of CFC sample at 25 ± 1°C for 7 days, which was found to be sufficient for attaining equilibrium. After the aqueous phase was separated by centrifugation at 10,000 rpm for 10 minutes, the γ-activity of the supernatant was measured with a well-type NaI(Tl) scintillation counter. The radioisotopes ^{137}Cs, ^{22}Na, ^{85}Sr, ^{60}Co, ^{152}Eu, ^{237}U, and ^{241}Am were used as tracers. The concentration of carrier-free ^{241}Am used for the distribution experiments was 2.1×10^{-9} M. The radioisotope ^{85}Sr was produced by the $^{86}Sr(\gamma,n)^{85}Sr$ reaction with 50 MeV bremsstrahlung from an electron accelerator (LINAC) in the Laboratory of Nuclear Science, Tohoku University, and was dissolved with 0.1 M HNO_3. Uranium-237 was prepared by the $^{238}U(\gamma,n)^{237}U$ reaction and purified by TBP extraction (18).

The uptake percentage of metal ions removed from the solution, R (%), and the distribution coefficient, K_d (cm^3/g), are defined as

$$R = [(A_i - A_t)/A_i] \times 100 \qquad (\%) \qquad (1)$$

$$K_d = [(A_i - A_f)/A_f] \times V/m \qquad (cm^3/g) \qquad (2)$$

where A_i, A_t, and A_f (cpm/cm^3) are the counting rates at the initial stage, at time t, and at equilibrium, respectively; m (g) is the weight of the CFC sample; and V (cm^3) is the volume of the aqueous phase.

Breakthrough Curve

The CFC-III (14–20 mesh) sample (3 g) was densely packed into a glass column (6 mm ϕ × 200 mm long) with a jacket thermostated at 20°C. The column volume of CFC-III was 3.4 cm^3. A feed solution containing 5×10^{-3} M Cs^+–5 M $NaNO_3$ was then passed through the column at a flow rate of 0.13 cm^3/min [space velocity (SV) = 2.3/h]. Every 3 cm^3 of the effluent was taken by a fraction collector, and then their γ-activities and pH were measured. A breakthrough curve was obtained by plotting the breakthrough ratio (C/C_0) against the effluent volume, where C_0 and C (cpm/cm^3) are the counting rates of the initial solution and the effluent, respectively.

RESULTS AND DISCUSSION

Surface Morphology and Structure

A cross section of the CFC-III particles embedded in the acrylic resin was submitted to EPMA. An energy dispersive spectroscopic (EDS) spectrum for the inner part of this particle is shown in Fig. 2. The constitutional elements of KNiFC (K, Fe, and Ni) were detected in the spectrum, indicating that the

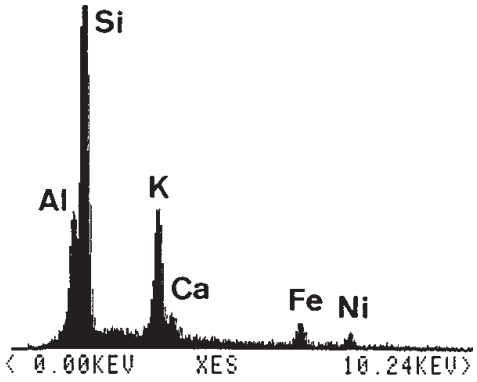

FIG. 2 EDS spectrum for inner part of CFC-III particle.

KNiFC crystals are loaded on the macropores of chabazite. Here the K^+ ions are constituents of both chabazite and KNiFC as exchangeable cations. The EDS spectrum in the vicinity of the surface was similar to that of the inner part of the particle. The chemical composition of CFC-III was determined to be $K_{1.45}Ni_{0.27}[NiFe(CN)_6]$ by quantitative EDS analysis using the ZAF correction method (19). Figure 3 shows the SEM image of the CFC-III parti-

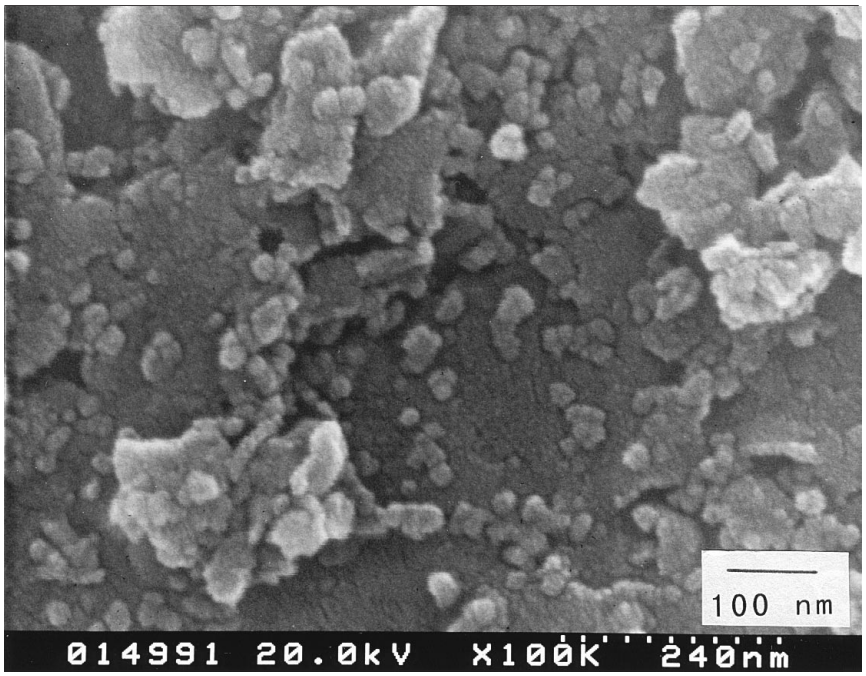

FIG. 3 SEM image of CFC-III particle.

cle. The KNiFC crystals are seen to be precipitated onto the surface of the carrier (chabazite) and are identically spherical/cubic in shape. The crystal size as roughly estimated from SEM image was about 20 nm. In order to check the homogeneity of loading of KNiFC, a loaded sample was further contacted with 0.1 M $CsNO_3$–5 M $NaNO_3$ solution, and the treated specimen was submitted to EPMA. Here the Cs^+ ions were preferentially adsorbed on KNiFC crystals. The result of line analysis of Cs-L_α for the cross section of the CFC granule showed that Cs^+ ions are uniformly dispersed throughout the granule, indicating loading of the KNiFC crystals onto the macropores.

Though the XRD intensity of the KNiFC crystals loaded was rather weak, main diffraction peaks for the face-centered cubic (FCC) structure of KNiFC, e.g., 200 ($2\theta = 17.620°$), 220 (24.740°), 222 (30.780°), and 400 (35.700°), were observed, together with those of chabazite. The lattice parameter of KNiFC was calculated to be 1.00163 ± 0.01167 nm (20), which is close to that of those prepared by precipitation methods (10). The structure of chabazite was unaltered before and after loading of KNiFC.

Physicochemical properties of the CFC samples are summarized in Table 1. The loading percentage for CFC-I prepared with 1 M $Ni(NO_3)_2$ was found to be somewhat larger than that with 0.5 M $Ni(NO_3)_2$. The loading percentage tended to increase with repeated times of impregnation, and in the triple loading (CFC-III) it attained 13.4 wt%, which is about 35% lower than that of copper-hexacyanoferrate-loaded resins (RCuCF-III) (21). In this experiment the impregnation operation was stopped after the third loading, and it would be necessary to do more impregnations to estimate the maximum amount of KNiFC that could be loaded on CFC. The optical density (D) of the absorption spectrum assigned to the C≡N stretching vibration at 2,100 cm^{-1} also increased with repeated runs (22).

TABLE 1
Physicochemical Properties for CFC Samples

Samples	Loading percentage (wt%)	D^a	$Q_{max}{}^b$ (mmol/g)
Chabazite (carrier)	—	—	1.97
CFC-I [0.5 M $Ni(NO_3)_2$][c]	3.7	0.055	1.87
CFC-I [1 M $Ni(NO_3)_2$][d]	5.9	0.18	1.45
CFC-II [1 M $Ni(NO_3)_2$]	10.9	0.46	1.44
CFC-III [1 M $Ni(NO_3)_2$]	13.4	0.70	1.51

[a] Optical density ($D = \ln I_0/I$) of asymmetric CN^- stretching at 2,100 cm^{-1}.
[b] Maximum amounts of Cs^+ adsorbed (Q_{max}) were calculated from Langmuir plots.
[c] Single loading with 0.5 M $Ni(NO_3)_2$.
[d] Single loading with 1 M $Ni(NO_3)_2$.

MARCEL DEKKER, INC.
270 Madison Avenue, New York, New York 10016

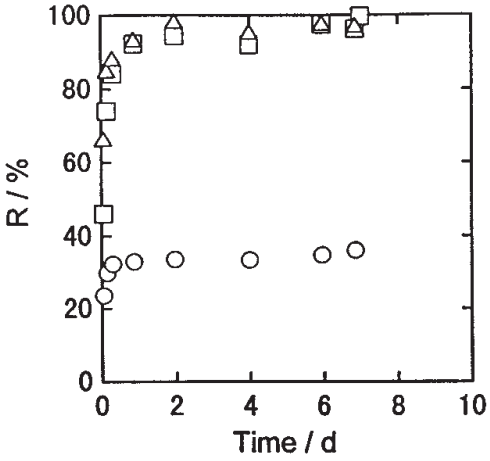

FIG. 4 Uptake rate of Cs^+ for chabazite and CFC-III. (○) Chabazite (14–20 mesh), (□) CFC-III (14–20 mesh), (△) CFC-III (65–100 mesh); *V/m*, 100 cm^3/g; 10 ppm Cs^+–5 M $NaNO_3$; centrifugation, 10^4 rpm, 10 minutes; 25°C.

Uptake Rate of Cs

Figure 4 shows the effect of equilibration time on the uptake percentage, *R* (%), of Cs^+ on chabazite and CFC-III in the presence of 5 M $NaNO_3$. Here the $NaNO_3$ concentration of 5 M corresponds to that in low-level radioactive waste solutions from the reprocessing process ([$NaNO_3$]: 400 g/dm^3) (23). The adsorption of Cs^+ on chabazite reached equilibrium within 3 hours, and a relatively low *R* value of about 35% was obtained. On the other hand, the adsorption of Cs^+ on CFC-III was fairly rapid in the initial stages, probably due to exchange on the surface, followed by a slow step controlled by mass transfer within particles (7, 10, 21). A relatively large *R* value, above 95%, was obtained within 2 days. The uptake rate for CFC-III with a particle size of 65–100 mesh was slightly faster than that with a larger particle size of 14–20 mesh.

Ion-Exchange Isotherm for Cs^+ Uptake

In order to clarify the ion-exchange mechanism, ion-exchange isotherms were obtained in a wide range of initial Cs^+ concentrations from 10^{-2} to 0.1 M. The equilibrium amount of Cs^+ adsorbed on CFC approached a constant value at Cs^+ concentrations above about 40 $mmol/dm^3$, suggesting that the uptake of Cs^+ follows a Langmuir-type adsorption equation (7, 10). The Langmuir equation is given by

$$Q_{eq} = KQ_{max}C_{eq}/(1 + KC_{eq}) \qquad \text{(mol/g)} \qquad (3)$$

where C_{eq} (mol/dm^3) and Q_{eq} (mol/g) are the equilibrium concentrations of

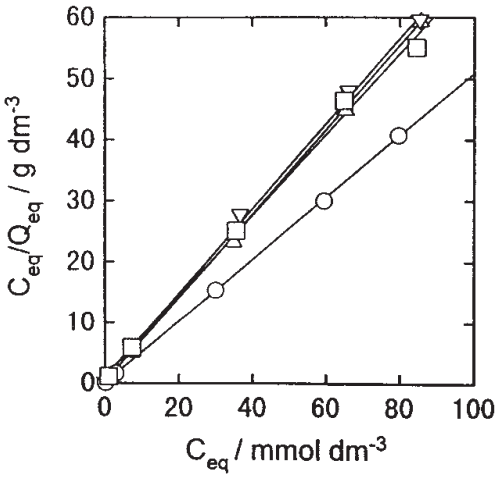

FIG. 5 Langmuir plots for Cs^+ uptake for chabazite and CFC. (○) Chabazite, (△) CFC-I, (▽) CFC-II, (□) CFC-III; pH_{eq} 3.70–5.83; equilibration, 25°C, 7 days.

Cs^+ in the aqueous and solid phases, respectively; Q_{max} (mol/g) is the maximum amount of Cs^+ taken up; and K (dm^3/mol) is the Langmuir constant. The equation can be rewritten as

$$C_{eq}/Q_{eq} = 1/KQ_{max} + (1/Q_{max})C_{eq} \qquad (g/dm^3) \tag{4}$$

As seen in Fig. 5, fairly linear relations between C_{eq}/Q_{eq} and C_{eq} were obtained from Langmuir plots, with correlation coefficients above 0.99. The estimated Q_{max} values are summarized in Table 1. The Q_{max} values for CFC were rather low compared with that for chabazite, suggesting that the macropores of chabazite were considerably blocked by the successive loading of KNiFC crystals; the Q_{max} value for CFC-III was about 25% lower than that for chabazite. No appreciable difference in Q_{max} values was observed among CFC samples prepared with 1 M $Ni(NO_3)_2$. The Q_{max} values for CFC were about 4–10 times larger than those for CuFC-loaded resins (21).

Distribution of Cs^+ in the Presence of Monovalent Cations

The effect of coexisting monovalent cations on $K_{d,Cs}$ was examined to estimate the selectivity to Cs^+. Figure 6 shows the effects of the initial concentration of competing monovalent cations (Na^+, K^+, and NH_4^+) on $K_{d,Cs}$ for CFC-III. Here the distribution behavior of Cs^+ for CFC-III is compared with that for chabazite.

The $K_{d,Cs}$ value for CFC-III was almost constant in a fairly wide range of Na^+ concentrations from 10^{-3} to 5 M; even at higher Na^+ concentration of

MARCEL DEKKER, INC.
270 Madison Avenue, New York, New York 10016

5 M, the $K_{d,Cs}$ value was above 10^4 cm^3/g, suggesting high selectivity to Cs^+. On the other hand, the $K_{d,Cs}$ for chabazite decreased linearly with increasing Na^+ concentration above 0.1 M, and the $K_{d,Cs}$ value for chabazite was considerably lowered below 10^2 cm^3/g in the presence of 5 M $NaNO_3$.

In the presence of K^+, the $K_{d,Cs}$ for CFC-III tended to decrease slightly with increasing K^+ concentration above 1 M. The distribution of Cs^+ for CFC-III was considerably affected by NH_4^+ concentration; there was a linearity with a slope of approximately -1 above 0.1 M in a plot of log $K_{d,Cs}$ vs log-$[NH_4^+]$, suggesting that the uptake of Cs^+ on KNiFC was substantially governed by a cation-exchange reaction of K^+ D Cs^+ (7, 24). In the presence of 5 M NH_4NO_3, the $K_{d,Cs}$ was considerably lowered below 10^2 cm^3/g; a highly concentrated NH_4^+ solution seems to be effective for the elution of Cs^+ adsorbed on CFC.

Based on Fig. 6, we can conclude that the order of $K_{d,Cs}$ in the presence of coexisting cations is $NH_4^+ > K^+ > Na^+$, which closely resembles the increasing order of the size of hydrated cations (25).

Distribution of Various Nuclides

The affinity of various radionuclides (^{137}Cs, ^{60}Co, ^{85}Sr, ^{152}Eu, ^{237}U, and ^{241}Am) for CFC-III was examined at different concentrations of $NaNO_3$. Table 2 summarizes the K_d values of various nuclides for chabazite and CFC-III at different concentrations of $NaNO_3$. A similar tendency was observed in the distribution behavior of radionuclides for chabazite; the K_d values were

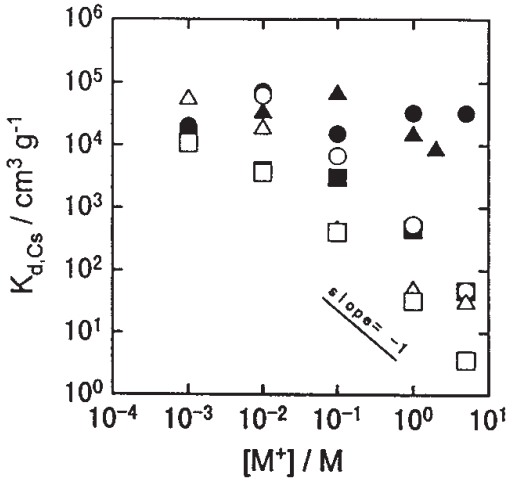

FIG. 6 Effects of initial concentration of monovalent cations on $K_{d,Cs}$ for chabazite and CFC-III. $M^+ = Na^+$, K^+, or NH_4^+; (●) Na^+/CFC-III, (▲) K^+/CFC-III, (■) NH_4^+/CFC-III, (○) Na^+/chabazite, (△) K^+/chabazite, (□) NH_4^+/chabazite.

TABLE 2
Comparison of K_d of Various Nuclides for Chabazite and CFC-III at Different Na^+ Concentrations

Ion exchanger	$[Na^+]$ (M)	K_d ($cm^3 \cdot g^{-1}$)					
		Cs	Sr	Am	Co	Eu	U
Chabazite	10^{-3}	1.1×10^4	7.7×10^3	2.0×10^3	1.4×10^4	2.4×10^4	1.1×10^3
	10^{-2}	6.3×10^4	3.6×10^3	1.6×10^3	6.6×10^3	1.5×10^4	1.3×10^3
	10^{-1}	6.8×10^3	2.0×10^2	4.2×10^2	1.9×10^2	3.3×10^3	8.7×10^2
	1	5.4×10^2	5.8	1.2×10	1.6×10	3.6×10	4.5×10^2
	5	4.9×10	—	3.0	1.0×10	1.4×10	3.4×10^2
CFC-III	10^{-3}	1.0×10^4	1.0×10^4	3.8×10^3	7.4×10^3	1.9×10^4	3.3×10^3
	10^{-2}	7.2×10^4	2.4×10^3	6.3×10^2	1.3×10^3	8.1×10^3	2.5×10^3
	10^{-1}	1.5×10^4	1.1×10^2	1.9×10^2	1.3×10^2	9.2×10^2	1.6×10^3
	1	3.3×10^4	2.4	1.3×10	6.4×10	3.9×10	8.6×10^2
	5	3.3×10^4	—	1.5×10	7.3×10	2.8×10	4.5×10^2

relatively large at concentrations of Na^+ below 10^{-2} M, beyond which they tended to decrease markedly with increasing Na^+ concentration. The K_d values of ^{137}Cs for chabazite were slightly larger than those for other nuclides because this zeolite has a relatively high selectivity to Cs^+ (17, 26). On the other hand, in the case of CFC-III there is a large difference between the K_d of ^{137}Cs and those of other nuclides; the $K_{d,Cs}$ value was almost constant above 10^4 cm^3/g up to 5 M Na^+, while those of other nuclides decreased with increasing Na^+ concentration, similar to the case of chabazite. The separation factors of Cs/Sr ($\alpha_{Cs/Sr} = K_{d,Cs}/K_{d,Sr}$) for CFC-III and chabazite at different concentrations of $NaNO_3$ can be estimated from Table 2. At concentrations of Na^+ below 10^{-2} M, there is little difference in $\alpha_{Cs/Sr}$ values between CFC-III and chabazite, while the difference becomes very large with increasing Na^+ concentration above 0.1 M. For example, the $\alpha_{Cs/Sr}$ value for CFC-III is calculated to be above 10^4 in the presence of 1 M Na^+, suggesting that this exchanger is available for the mutual separation of these nuclides.

Breakthrough Properties of Cs through CFC Column

To obtain information on the dynamic adsorption behavior of Cs^+, its breakthrough property from a highly concentrated $NaNO_3$ (5 M $NaNO_3$) solution was examined at a constant flow rate using the column packed with CFC-III. Figure 7 illustrates the breakthrough curve for Cs^+, which is a symmetrical S-shaped profile. This suggests no dislodgment of KNiFC from the matrix of chabazite. The pH values of the effluents in the initial stage were somewhat higher than that of the feed solution (5×10^{-3} M Cs^+–5 M $NaNO_3$, pH

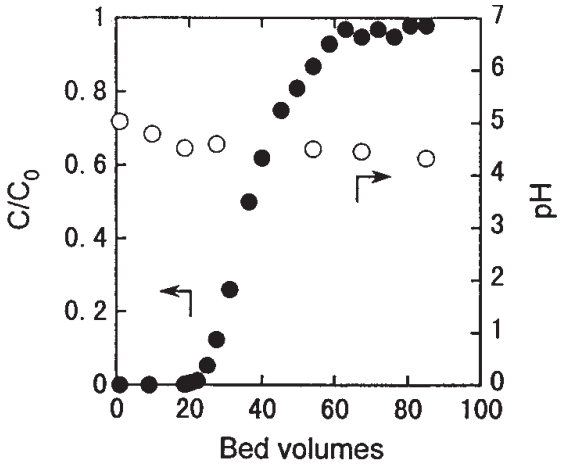

FIG. 7 Breakthrough curve for Cs^+ through a column packed with CFC-III. CFC-III, 3.00 g; feed, 5×10^{-3} M Cs^+–5 M $NaNO_3$; *SV*, 2.3/h; 20°C.

3.92) because the effluents contained exchangeable K^+ ions replaced with Cs^+ and Na^+. The break point of 5% breakthrough was estimated to be 84.6 cm^3 [bed volume (*BV*) = 24.9], which was about 2.5 times larger than that of chabazite. The breakthrough capacity (B.T.Cap.) and total capacity (T.Cap.) were calculated to be 0.14 and 0.21 meq/g, respectively, resulting in a relatively high column utilization (B.T.Cap./T.Cap.) of 67%. The column packed with CFC was thus effective for the selective removal of trace amounts of ^{137}Cs from waste solutions containing highly concentrated $NaNO_3$.

CONCLUSIONS

Potassium nickel hexacyanoferrates (KNiFC) were loaded on a porous matrix of granular chabazite by successive impregnations of $Ni(NO_3)_2$ and $K_4Fe(CN)_6$. The loading percentage of KNiFC increased with repetition impregnations. The loading of KNiFC on chabazite led to improvements in both mechanical stability and selectivity to Cs^+; the $K_{d,Cs}$ for CFC was almost independent of the coexisting $NaNO_3$ concentration, and a relatively large $K_{d,Cs}$ value above 10^4 cm^3/g was obtained even in the presence of 5 M $NaNO_3$. The CFC products also exhibited a relatively large separation factor of Cs/Sr above 10^4. Selective removal of Cs^+ from highly concentrated $NaNO_3$ solutions can be achieved by using a column packed with CFC.

ACKNOWLEDGMENTS

The authors express appreciation to Mr. T. Kamaya and Mr. Y. Sato (Tohoku University) for their helpful discussions of SEM and EPMA data.

REFERENCES

1. *IAEA Technical Report Series, No. 356* (1993).
2. M. Kubota, *High Level Radioactive Waste and Spent Fuel Management*, American Society of Mechanical Engineers, New York, NY, 1989, p. 537.
3. W. Faubel and A. Ali, *Radiochim. Acta*, *40*, 49 (1986).
4. E. H. Tusa, A. Paavola, R. Harjula, and J. Lehto, *Proceedings of the Symposium on Waste Management*, *Vol. 2*, Tucson, AZ, 1993, p. 1687.
5. J. Lehto, R. Harjula, E. Tusa, and A. Paavola, *Ibid.*, p. 1693.
6. C. Loos-Neskovic et al., *Talanta*, *31*, 1133 (1984).
7. H. Mimura, J. Lehto, and R. Harjula, *J. Nucl. Sci. Technol.*, *34*, 484 (1997).
8. H. Mimura, J. Lehto, and R. Harjula, *Ibid.*, *34*, 582 (1997).
9. H. Mimura, J. Lehto, and R. Harjula, *Ibid.*, *34*, 607 (1997).
10. H. Mimura, N. Kageyama, K. Akiba, M. Yoneya, and Y. Miyamoto, *Solv. Extr. Ion Exch.*, *16*, 1013 (1998).
11. K. Watari, K. Imai, and M. Izawa, *J. Nucl. Sci. Technol.*, *4*, 190 (1967).
12. V. I. Baranovskii, Ya. Viza, G. S. Katykhin, and M. K. Nikitin, *Radiokhimiya*, *9*, 698 (1967).
13. I. F. Karpova and E. V. Kazakov, *Vestn. Leningr. Univ., Ser. Fiz. Khim.*, *21*, 159 (1966).
14. N. Mishiro, A. Kamoshida, S. Kadoya, and T. Ishihara, *Nippon Genshiryoku Gakkaishi*, *6*, 2 (1964).
15. K. Terada, H. Hayakawa, K. Sawada, and T. Kiba, *Talanta*, *17*, 955 (1970).
16. D. W. Breck, *Zeolite Molecular Sieves*, Krieger Publishing, Florida, 1974, p. 138.
17. H. Mimura and T. Kanno, *J. Nucl. Sci. Technol.*, *22*, 284 (1985).
18. K. Akiba et al., *J. Radioanal. Chem.*, *7*, 203 (1971).
19. S. J. B. Reed, Electron Microprobe Analysis, Cambridge University Press, Cambridge, 1993.
20. D. E. Williams, *Ames Laboratory Report*, *IS-1052*, Institute for Physical Research and Technology, Iowa State University, Ames, IA, 1964.
21. I. J. Singh and B. M. Misra, *Sep. Sci. Technol.*, *31*, 1695 (1996).
22. T. Ceranic, *Z. Naturforsch.*, *33(b)*, 1484 (1978).
23. I. Kobayashi et al., *1997 Fall Meeting of the Atomic Energy Society of Japan*, 1997, p. 751.
24. T. Ceranic, D. Trifunovic, and R. Adamovic, *Z. Naturforsch.*, *33(b)*, 1099 (1978).
25. H. A. Laitinen and W. E. Harris, *Chemical Analysis*, McGraw-Hill Kogakusha, Tokyo, 1975.
26. Ref. 16, p. 555.

Received by editor February 19, 1998
Revision received May 1998

Request Permission or Order Reprints Instantly!